

Conformational Study on Various Tripeptides Containing Threonine: A Density Functional Theory Approach

Manoj Kumar Shrestha^{1,2,*}, Nabin Dawadi³, Mani Raj Shrestha⁴, Pukar Sedai¹, Sudip Adhikari¹, Hari Prasad Lamichhane⁵

¹ Department of Physics, Amrit Campus, Tribhuvan University, Kathmandu, Nepal

² Department of Physics and Astronomy, Wayne State University, Detroit, MI, USA

³ Department of Physics, Patan Multiple Campus, Tribhuvan University, Kathmandu, Nepal

⁴ Department of Microbiology, Tri-Chandra Multiple Campus, Tribhuvan University, Kathmandu, Nepal

⁵ Central Department of Physics, Tribhuvan University, Kathmandu, Nepal

*Email: manoj_shrestha@wayne.edu

(Received: September 19, 2025, Received in revised form: November 22, 2025, Accepted: December 8, 2025, Available online: December 19, 2025)

DOI: <https://doi.org/10.3126/arj.v6i1.87495>

Highlights

- Eight tripeptides with central threonine were constructed and analyzed using Density Functional Theory
- Geometry optimizations and calculations were carried out in Gaussian 03 using the B3LYP functional with 6-31G* and 6-311G* basis sets
- The Methionine-Threonine-Phenylalanine tripeptide exhibited the lowest total energy among the studied tripeptides, indicating high conformational stability
- Internal rotation barriers in threonine were determined via potential energy surface calculations

Abstract

Density functional theory (DFT) calculations were performed using B3LYP/6-31G* and B3LYP/6-311G* basis sets to investigate the conformational stability of eight tripeptides containing threonine. Each peptide was constructed with threonine flanked by varied amino acids at N- and C-termini including alanine (Ala), arginine (Arg), asparagine (Asn), cysteine (Cys), methionine (Met), aspartic acid (Asp), proline (Pro), serine (Ser) and phenylalanine (Phe). Methionine- Threonine-Phenylalanine showed the lowest total energy ($-1029601 \text{ kcal}\cdot\text{mol}^{-1}$ for 6-31G*, $-1029809 \text{ kcal}\cdot\text{mol}^{-1}$ for 6-311G*). Maximum deviations in bond length (0.053 \AA) and bond angle (1.8°) were observed for Proline-Threonine-Serine. Significant α -carbon bond angle deviations of 4.4° and 3.4° were found for Methionine-Threonine-Phenylalanine and Lysine-Threonine-Methionine, respectively. Potential energy surface scans of threonine revealed rotational energy barriers of $6.914 \text{ kcal}\cdot\text{mol}^{-1}$ ($-\text{NH}_2$), $12.711 \text{ kcal}\cdot\text{mol}^{-1}$ ($-\text{COOH}$), and $8.648 \text{ kcal}\cdot\text{mol}^{-1}$ ($-\text{CH}(\text{CH}_3)\text{OH}$) group. This study highlights how amino acid sequence influences peptide conformation and intramolecular interactions, contributing to a deeper understanding of protein structure and energetics.

Keywords: threonine, tripeptide, DFT calculation, potential energy scan

Introduction

Proteins are complex macromolecules responsible for a wide array of biological functions, including catalysis, transport, signaling, and structural support. The function of a protein is intricately related to its three-dimensional structure, which is

*Corresponding author

ultimately determined by the amino acid sequence and the physicochemical properties of its constituent residues (Lehninger et al., 2005; Voet et al., 2016). Short peptides such as dipeptides and tripeptides serve as effective models for studying local structural preferences in proteins. Tripeptides are particularly useful in exploring how the nature and position of amino acids influence the overall conformational behavior of peptides (Garrett, 2015; Hardin and Luthey-Schulten, 2002). These studies help us understand the backbone flexibility, steric hindrance, and hydrogen-bonding patterns of individual residues in a simplified yet relevant context.

Threonine (Thr) is of particular interest because of its polar side chain bearing a hydroxyl group, which can form hydrogen bonds and alter the local geometry of the peptide chain (Wagner and Musso, 1983; Barrett and Elmore, 1998). The orientation and conformational flexibility of the side chain in threonine make it a crucial residue in determining structural motifs in proteins such as turns and helices.

Numerous theoretical studies have used model peptides composed of glycine and alanine due to their minimal steric bulk and structural simplicity, which make them ideal systems for understanding peptide backbone conformations (Kaschner and Hohl, 1998; Selvarangan and Kolandaivel, 2004; Yakubovich et al., 2006). However, tripeptides containing threonine have not been extensively studied with higher-level quantum chemical methods, in part because they have many low-energy conformations and the threonine side-chain hydroxyl adds extra rotamers and intramolecular hydrogen-bonding patterns, which greatly increases computational cost, especially when solvent is considered. Earlier works have examined peptides using Hartree–Fock and molecular mechanics approaches (Hardin and Luthey-Schulten, 2002; Chasse et al., 2001), whereas density functional theory (DFT) provides a more accurate and efficient way to analyze electronic and geometric structure (Kaschner and Hohl, 1998; Yakubovich et al., 2006; Mondal et al., 2007; Subedi, 2017). It is also widely used to interpret vibrational features of amino-acid side chains (Sjöberg et al., 2014).

The present work employs DFT using B3LYP functional with two basis sets, 6-31G* and 6-311G*, to explore the structural features of eight tripeptides containing threonine at various positions. Key geometrical parameters such as bond lengths, bond angles, dihedral angles, and torsional barriers are examined to determine how neighboring residues affect conformational stability and side-chain flexibility. The results aim to enhance our understanding of sequence- dependent conformational variation, which may contribute to better modeling of peptide-based biomolecular systems. The B3LYP function was employed because it is widely validated for peptide conformational analysis and provides a consistent framework for comparing residue dependent structural variations. Although using multiple functionals (such as M06-2X or ω B97x-D) could provide additional benchmarking, such extensions are outside the scope of the present work and are proposed for future studies.

Materials and Methods

Computational Details

In this study, eight tripeptides incorporating threonine as the central residue were constructed to investigate the conformational dependence on varying side-chain amino acid residues. These peptides were designed by combining threonine with different amino acids like alanine, arginine, asparagine, cysteine, methionine, aspartic acid, proline, serine and phenylalanine, at both the N- and C-termini.

All molecular models were constructed using GaussView (Dennington et al., 2008) whereas geometry optimization as well as vibrational frequency analysis were carried out in Gaussian 03 (Frisch et al., 2004). Density Functional Theory (DFT) was used for calculations with employed hybrid B3LYP functional with two basis sets: 6-31G* and 6-311G*. This comparative approach allowed for assessment of computational accuracy across basis sets (Lee et al., 1988; Foresman and Frisch, 1996). All optimized structures are shown in Fig. 1 and were verified by ensuring the absence of imaginary frequencies, confirming true local minimum on the potential energy surface.

To facilitate consistent structural analysis, a fixed atom numbering scheme was used for each optimized tripeptide. This enabled the systematic labeling of bond lengths and bond angles across all structures, aiding comparative analysis. The atom index mapping used in this study for labeling the structural parameters like bond lengths (a – j), bond angles (I – XII), dihedral angles (D_1 – D_2 , D_{Nx} , D_{Ny}), and α -carbon geometry (k – p) is provided in the supplementary information (Table S1, Table S2, Table S3, Table S4).

Structural parameters such as bond lengths, bond angles, dihedral angles, and α -carbon geometry were evaluated. In addition, potential energy scans (PES) were performed for internal rotation around -NH₂, -COOH, and the side chain -CH(CH₃)OH of

threonine to evaluate intramolecular rotational barriers. C-terminus amino acids and N-terminus amino acids added in threonine are hereafter named as X and Y amino acids, respectively.

Results and Discussion

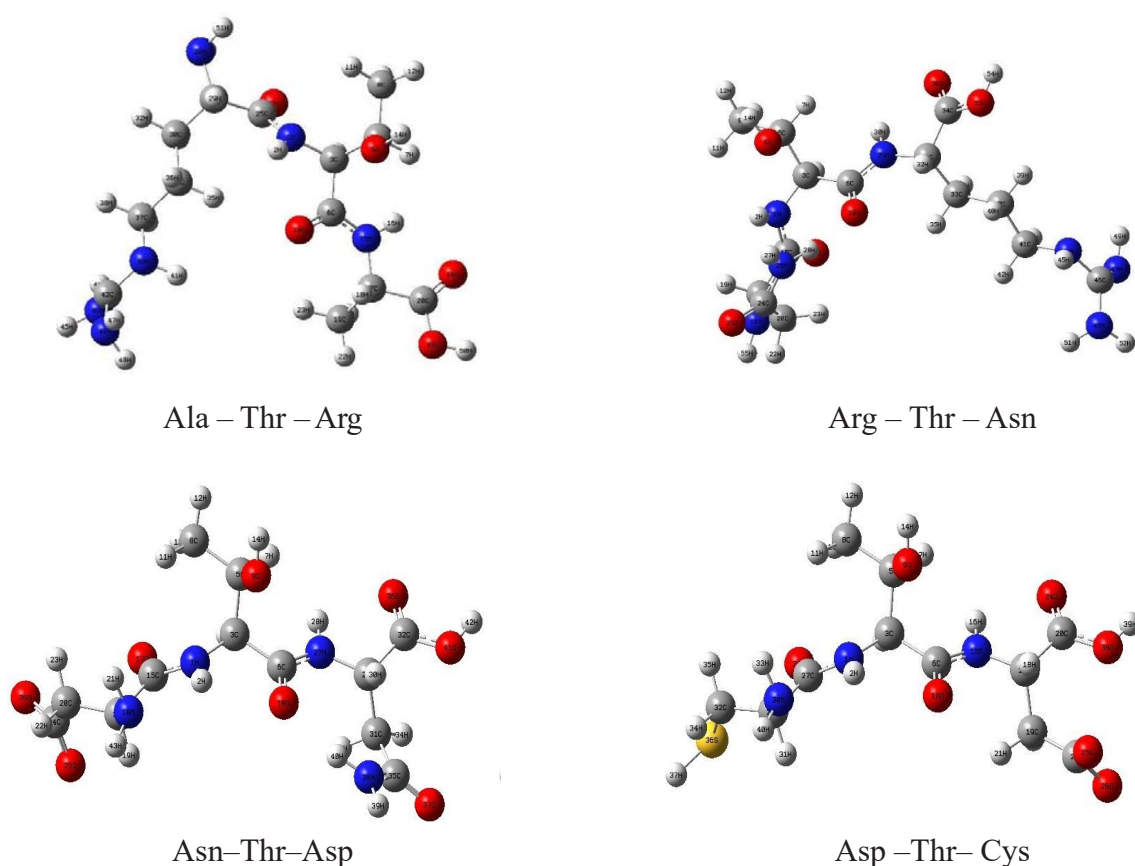
The total energies of all eight optimized tripeptides, calculated at both B3LYP/6-31G* and B3LYP/6-311G* levels, are presented in Table 1 and visualized in Fig. 2. The 6-311G* basis set consistently yielded lower (more stable) energies, and therefore all subsequent structural analyses are based on geometries optimized at the B3LYP/6-311G* level of theory.

Bond lengths and Bond angles

The optimized geometries of the threonine-containing tripeptides show that backbone amide parameters fall within the expected ranges for peptides. In particular, the observed C=O and C–N bond lengths reflect the resonance stabilization characteristic of the peptide bond (Pauling, 1960) and are consistent with typical linkage geometry in protein structures (Barden and Tooze, 2012).

Among the studied combinations, the Proline-Threonine-Serine tripeptide exhibited the largest deviation, with a maximum bond length variation of 0.053 Å and bond angle deviation of 1.8°. This is likely due to the conformational rigidity introduced by the cyclic nature of proline and the hydrogen bonding propensity of serine (MacArthur and Thornton, 1991; Berg et al., 2007). Deviations in the bond angles around the α -carbon were particularly significant in the Methionine-Threonine-Phenylalanine and Lysine-Threonine-Methionine combinations, with maximum angular deviations of 4.4° and 3.4°, respectively. These distortions can be attributed to steric hindrance and side chain bulkiness that affect the ideal tetrahedral geometry at the α -carbon center (Mondal et al., 2007; Ramachandran et al., 1963).

A full summary of the bond lengths and angles observed across all tripeptides are presented in Table 2 and Table 3. These findings highlight the influence of neighboring residues on local peptide geometry and suggest that small changes in side chain properties can lead to measurable structural effects that may contribute to broader conformational behavior in proteins.



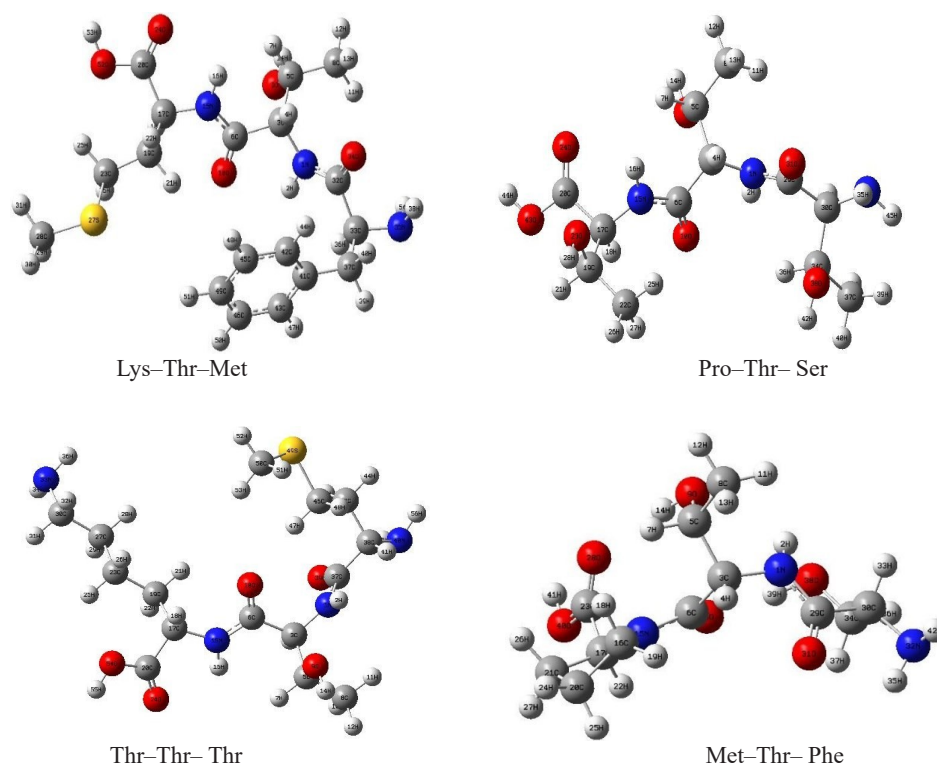


Fig. 1. Energy optimized structures of the tripeptides with DFT-B3LYP/6-311G*.

Table 1: Calculated energy ($\text{kcal}\cdot\text{mol}^{-1}$) of all the tripeptides.

| Tripeptide Combination | Calculated energy ($\text{kcal}\cdot\text{mol}^{-1}$) | |
|------------------------|---|-------------------|
| | DFT-B3LYP/6-31G* | DFT-B3LYP/6-311G* |
| Ala-Thr-Arg | -763201 | -763399 |
| Arg-Thr-Asn | -869061 | -869287 |
| Asn-Thr-Asp | -809179 | -809394 |
| Asp-Thr-Cys | -953179 | -953380 |
| Met-Thr-Phe | -1029601 | -1029809 |
| Thr-Thr-Thr | -729138 | -729330 |
| Lys-Thr-Met | -993666 | -993872 |
| Pro-Thr-Ser | -681187 | -681366 |

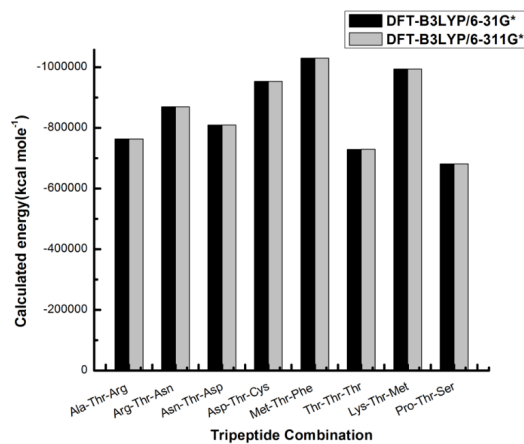


Fig. 2. Calculated energy of the tripeptides by DFT-B3LYP method using 6-31G* and 6-311G* basis sets.

Table 2: The calculated bond lengths of amide planes for 8 tripeptides studied. [Alphabetical labels: X- amino acid (i.e., a – e) and Y-amino acid (i.e., f – j) are based on the Fig. 1]

| X-amino acid | Bond length (Å) | | | | | Y-amino acid | Bond length (Å) | | | | |
|----------------|-----------------|-------|-------|-------|-------|----------------|-----------------|-------|-------|-------|-------|
| | a | b | c | d | e | | f | g | h | i | j |
| Ala | 1.453 | 1.010 | 1.358 | 1.221 | 1.544 | Arg | 1.541 | 1.224 | 1.365 | 1.009 | 1.447 |
| Arg | 1.455 | 1.010 | 1.353 | 1.225 | 1.549 | Asn | 1.535 | 1.221 | 1.366 | 1.011 | 1.444 |
| Asn | 1.454 | 1.011 | 1.352 | 1.226 | 1.540 | Asp | 1.540 | 1.223 | 1.353 | 1.012 | 1.444 |
| Asp | 1.448 | 1.010 | 1.363 | 1.218 | 1.541 | Cys | 1.540 | 1.224 | 1.356 | 1.012 | 1.444 |
| Met | 1.451 | 1.010 | 1.358 | 1.220 | 1.541 | Phe | 1.538 | 1.226 | 1.361 | 1.012 | 1.449 |
| Thr | 1.445 | 1.008 | 1.362 | 1.220 | 1.542 | Thr | 1.539 | 1.218 | 1.367 | 1.009 | 1.445 |
| Lys | 1.454 | 1.010 | 1.359 | 1.220 | 1.549 | Met | 1.534 | 1.222 | 1.363 | 1.008 | 1.444 |
| Pro | 1.460 | 1.070 | 1.359 | 1.229 | 1.538 | Ser | 1.534 | 1.224 | 1.368 | 1.014 | 1.445 |
| Average | 1.453 | 1.017 | 1.358 | 1.222 | 1.543 | Average | 1.538 | 1.223 | 1.362 | 1.011 | 1.445 |
| Max. deviation | 0.008 | 0.053 | 0.006 | 0.007 | 0.006 | Max. deviation | 0.004 | 0.005 | 0.009 | 0.003 | 0.004 |

Table 3: The calculated bond angles of amide planes for 8 tripeptides studied. [Roman labels: X-amino acid (i.e. I – VI) and Y-amino acid (i.e., VII – XII) are based on the Fig. 1]

| X-amino acid | Bond angle (°) | | | | | | Y-amino acid | Bond angle (°) | | | | | |
|----------------|----------------|-------|-------|-------|-------|-------|----------------|----------------|-------|-------|-------|-------|-------|
| | I | II | III | IV | V | VI | | VII | VIII | IX | X | XI | XII |
| Ala | 116.2 | 121.8 | 120.9 | 122.8 | 115.1 | 122.1 | Arg | 121.0 | 116.5 | 122.7 | 119.3 | 121.7 | 117.8 |
| Arg | 116.2 | 122.5 | 121.2 | 122.2 | 114.6 | 123.2 | Asn | 121.6 | 116.2 | 122.2 | 119.0 | 119.7 | 117.1 |
| Asn | 116.1 | 122.0 | 121.3 | 122.9 | 115.4 | 121.7 | Asp | 120.7 | 114.8 | 124.5 | 117.7 | 122.0 | 118.6 |
| Asp | 116.0 | 121.3 | 121.2 | 122.3 | 115.1 | 122.6 | Cys | 121.6 | 114.5 | 123.9 | 117.8 | 121.9 | 118.3 |
| Met | 116.9 | 121.4 | 121.5 | 122.7 | 115.3 | 122.0 | Phe | 120.7 | 116.1 | 123.2 | 119.7 | 121.8 | 116.7 |
| Thr | 115.4 | 121.7 | 119.6 | 123.0 | 115.1 | 121.9 | Thr | 122.4 | 114.7 | 122.9 | 119.5 | 121.6 | 118.0 |
| Lys | 116.4 | 122.1 | 121.5 | 122.7 | 114.6 | 122.8 | Met | 120.9 | 115.3 | 122.8 | 119.9 | 121.6 | 116.2 |
| Pro | 115.7 | 121.8 | 120.4 | 122.2 | 115.6 | 121.8 | Ser | 122.1 | 115.3 | 122.6 | 116.4 | 119.4 | 117.4 |
| Average | 116.1 | 121.8 | 121.0 | 122.6 | 115.1 | 122.3 | Average | 121.4 | 115.4 | 123.1 | 118.7 | 121.2 | 117.5 |
| Max. deviation | 0.8 | 0.7 | 1.4 | 0.4 | 0.8 | 0.9 | Max. deviation | 0.9 | 1.1 | 0.9 | 1.2 | 1.8 | 1.3 |

α – Carbon Geometry: In addition to the analysis of amide bond parameters, we examined the geometry around the central α -carbon atoms of threonine in each tripeptide to assess how side- chain variation at the N- and C-termini influences local backbone conformation. In ideal tetrahedral geometry, the bond angles around an sp^3 -hybridized α -carbon approach 109.5°. However, deviations are expected in peptides due to steric constraints and intramolecular interactions.

Among the eight tripeptides studied, significant angular distortions were observed in both X- group and Y-group bond angles around the threonine α -carbon. The largest deviation in the X- group was 4.4° and 3.7° in Methionine-Threonine-Phenylalanine, followed by 2.2° in Proline-Threonine-Serine. Similarly, the maximum Y- group deviation was 3.4° for Lysine-Threonine-Methionine, with notable deviations of 2.7° in Aspartic-Threonine-Cysteine. In contrast, the Alanine-Threonine-Arginine tripeptide consistently showed minimal deviation in both groups within 1.7° of the averages. These variations can be attributed to the steric hindrance imposed by bulkier residues such as methionine, phenylalanine, proline, and lysine, which distort the tetrahedral configuration at the α -carbon (Mondal et al., 2007; Ramachandran et al., 1963).

These findings underscore how α -carbon bond angles can be significantly modulated by adjacent residues. Such variations are not only structurally relevant but can also propagate through the peptide chain, potentially influencing folding behavior, secondary structure preferences, and overall conformational stability (Branden and Tooze, 2012). The complete angular data for all tripeptides studied are summarized in Table 4.

Table 4: Calculated α -carbon bond angles ($^{\circ}$) in both terminal residues of all tripeptides studied. [Alphabetical labels: X-amino acid (i.e., k – m) and Y-amino acid (i.e., n – p) are based on the Fig. 1]

| X-amino acid | Bond angle ($^{\circ}$) | | | Y-amino acid | Bond angle ($^{\circ}$) | | |
|----------------|---------------------------|-------|-------|----------------|---------------------------|-------|-------|
| | k | l | m | | n | o | p |
| Ala | 112.8 | 108.5 | 107.5 | Arg | 111.5 | 109.7 | 110.1 |
| Arg | 111.4 | 108.4 | 106.7 | Asn | 106.8 | 109.6 | 109.3 |
| Asn | 114.1 | 108.4 | 107.0 | Asp | 111.4 | 105.1 | 109.3 |
| Asp | 111.6 | 109.5 | 107.4 | Cys | 110.3 | 105.7 | 110.7 |
| Met | 107.1 | 108.5 | 111.2 | Phe | 111.7 | 110.0 | 109.9 |
| Thr | 112.9 | 107.3 | 109.1 | Thr | 107.7 | 108.1 | 109.0 |
| Lys | 111.3 | 108.5 | 106.9 | Met | 106.4 | 109.4 | 109.8 |
| Pro | 110.5 | 111.0 | 103.9 | Ser | 112.9 | 109.4 | 109.3 |
| Average | 111.5 | 108.8 | 107.5 | Average | 109.8 | 108.4 | 109.7 |
| Max. Variation | 4.4 | 2.2 | 3.7 | Max. Variation | 3.4 | 2.7 | 1.0 |

Dihedral angle: Dihedral angle analysis was performed to assess the planarity of the amide plane in the studied tripeptides. Table 5 shows the dihedral angle of the amide plane for the tripeptide studied. Each structure contains two amide planes: one adjacent to the X-amino group and the other to the Y-amino group, with dihedral angles labeled as D_1 , D_2 , D_3 , D_{N_x} (X-side) and D_4 , D_5 , D_6 , D_{N_y} (Y-side) (Fig. 1). In perfectly planar geometry, D_1 , D_2 , D_{N_x} , D_4 , D_5 , and D_{N_y} should be 180° (or -180°), while D_3 and D_6 should be 0° .

Table 6 lists the deviations of D_{N_x} and D_{N_y} from 180° , along with backbone torsion angles ϕ and ψ . The largest deviation in D_{N_x} (17.2°) occurred in Thr – Thr – Thr, while the largest deviation in D_{N_y} (33.8°) was observed in Pro – Thr – Ser, indicating non-planarity at the amide nitrogen. ϕ and ψ varied across terminal –R groups, but no consistent trend was identified. These deviations are attributed to hydrogen bonding and steric interactions between –R group atoms and amide plane hydrogens. In Thr – Thr – Thr, interatomic distances 10O – 18H, 15N – 4H, 15H – 7N, and 1N – 33H were 2.353 Å, 2.680 Å, 2.741 Å, and 2.568 Å, respectively. In Pro – Thr – Ser, distances 1N – 33H, 1N – 39H, and 31O – 4H were 2.622 Å, 2.651 Å, and 2.508 Å, confirming strong hydrogen bonding in these peptides. Such interactions correlate with the observed maximum deviations, influencing conformational flexibility and overall geometry (Mondal et al., 2007).

Table 5: Calculated dihedral angles ($^{\circ}$) of the amide plane for all the tripeptides studied. [Atom numbering is based on the Fig. 1]

| X-amino acid | Dihedral angle ($^{\circ}$) | | | | Y-amino acid | Dihedral angle ($^{\circ}$) | | | |
|--------------|-------------------------------|--------------------|------------------|------------------------|--------------|-------------------------------|--------------------|------------------|------------------------|
| | $D_1(180^{\circ})$ | $D_2(180^{\circ})$ | $D_3(0^{\circ})$ | $D_{N_x}(180^{\circ})$ | | $D_4(180^{\circ})$ | $D_5(180^{\circ})$ | $D_6(0^{\circ})$ | $D_{N_y}(180^{\circ})$ |
| Ala | 179.4 | 173.1 | 5.5 | 167.6 | Arg | 179.2 | 170.5 | 11.6 | 158.9 |
| Arg | 179.8 | 179.7 | -2.9 | -177.4 | Asn | 178.6 | 168.1 | 14.6 | 153.6 |
| Asn | 179.9 | 172.6 | 2.4 | 170.2 | Asp | -179.1 | 169.2 | 4.2 | 165.0 |
| Asp | 179.3 | 171.4 | 5.6 | 165.7 | Cys | -179.3 | 168.7 | 3.7 | 164.9 |
| Met | 179.5 | 177.3 | 2.4 | 174.9 | Phe | 178.1 | 169.6 | 14.0 | 155.6 |
| Thr | 179.4 | 168.3 | 5.5 | 162.8 | Thr | -179.7 | 165.1 | 9.0 | 156.2 |
| Lys | 179.1 | -179.3 | -0.5 | -178.8 | Met | 179.8 | 171.7 | 9.5 | 162.2 |
| Pro | -172.7 | 162.4 | 60.7 | -176.9 | Ser | -177.4 | 160.6 | 14.5 | 146.2 |

Table 6: Calculated deviation from 180° in 'D' and the corresponding value of $\varphi(^{\circ})$ and $\psi(^{\circ})$ in all the tripeptides studied. [Atom numbering is based on the Fig. 1]

| X-amino acid | -R group | D (deviation from 180°) | $\varphi(^{\circ})$ | Y-amino acid | -R group | D (deviation from 180°) | $\psi(^{\circ})$ |
|--------------|--|----------------------------|---------------------|--------------|--|----------------------------|------------------|
| Ala | CH ₃ | 12.4 | -153.2 | Arg | (CH ₂) ₃ (NH)C(NH ₂) ₂ | 21.1 | 140.6 |
| Arg | (CH ₂) ₃ (NH)C(NH ₂) ₂ | 2.6 | -156.3 | Asn | CH ₂ CONH ₂ | 26.4 | 150.3 |
| Asn | CH ₂ CONH ₂ | 9.8 | -158.0 | Asp | CH ₂ COOH | 15.0 | 22.6 |
| Asp | CH ₂ COOH | 14.3 | -159.8 | Cys | CH ₂ SH | 15.1 | 26.6 |
| Met | (CH ₂) ₂ SCH ₃ | 5.1 | -155.2 | Phe | CH ₂ Ph | 24.4 | 123.9 |
| Thr | CHCH ₃ OH | 17.2 | -120.2 | Thr | CHCH ₃ OH | 23.8 | 156.0 |
| Lys | (CH ₂) ₄ NH ₂ | 1.2 | -156.5 | Met | (CH ₂) ₂ SCH ₃ | 17.8 | 132.7 |
| Pro | (CH ₂) ₃ | 3.1 | -59.0 | Ser | CH ₂ OH | 33.8 | 164.5 |

Potential Energy Scan (PES) of Threonine (Barriers to Rotation)

The internal rotational barriers of the threonine residue were investigated by performing potential energy scans on three groups: (a) amino (–NH₂), (b) carboxyl (–COOH), and (c) side-chain R (–CH(CH₃)OH). The threonine geometry was first optimized at the DFT-B3LYP/6-311G* level, after which each group was rotated from –180° to +180° in 10° increments, keeping the remainder of the molecule fixed. The dihedral angles for the rotation of –NH₂, –COOH and –CH(CH₃)OH groups are the angle of atoms 6C and 2H with respect to the bond 1N-3C, the angle of atoms 1N and 10O with respect to the bond 6C-3C and of atoms 6C and 9O with respect to the bond 5C-3C respectively keeping the rest of the part of threonine molecule fixed. The energy curves for all three-group rotations of threonine are given in Fig. 3, Fig. 5, and Fig. 7 respectively.

The plot in Fig. 3 shows Potential energy scan while Fig. 4 shows conformers of the –NH₂ group in threonine, defined by the dihedral angle between atoms 6C and 2H relative to bond 1N-3C, revealed two low-energy conformers, B (–60°; –275086.329 kcal·mol^{–1}) and D (60°; –275086.087 kcal·mol^{–1}), separated by rotational barriers of 6.914 and 1.588 kcal·mol^{–1} for B, and 1.346 and 7.466 kcal·mol^{–1} for D. High-energy conformers A (180°), C (0°), and E (150°) corresponded to –275079.415 kcal·mol^{–1}, –275084.741 kcal·mol^{–1}, and –275078.621 kcal·mol^{–1}, respectively. The barrier magnitudes obtained from our DFT-B3LYP/6-311G* calculations indicate significantly hindered rotation of the –NH₂ group in threonine, in line with the constrained internal motions reported in conformational studies of threonine (Barone et al., 2023).

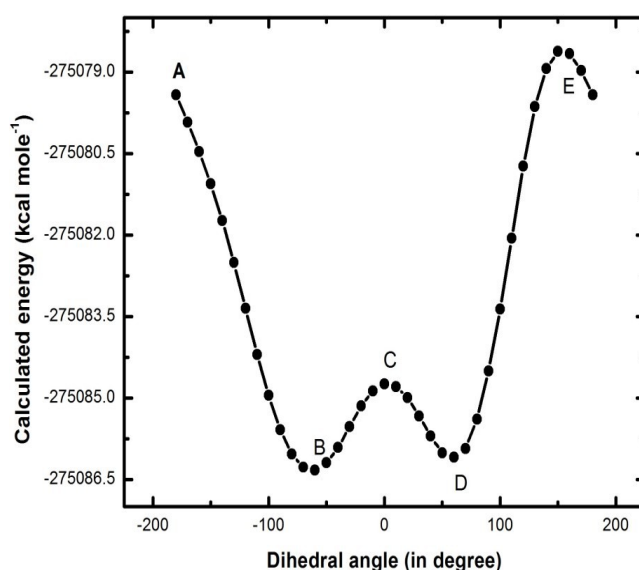


Fig. 3: Energy curve for the rotation of –NH₂ group in threonine.

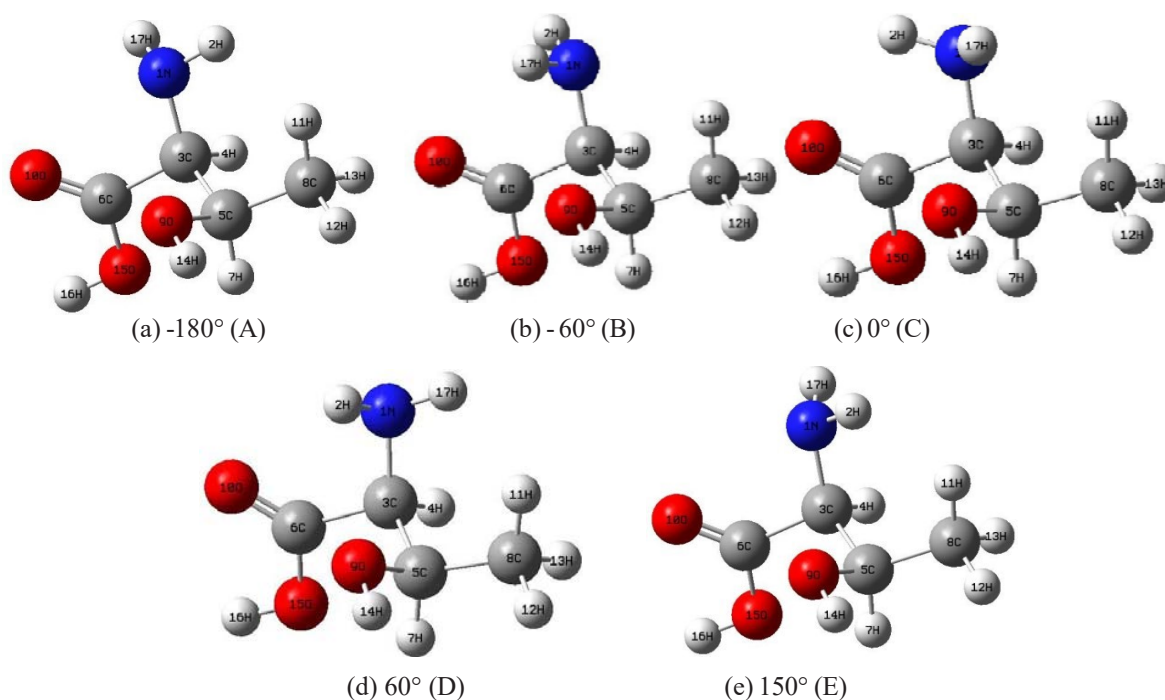


Fig. 4. Conformations obtained for the potential energy scan study of threonine while rotating $-\text{NH}_2$ group at different angles (a)-180°, (b)-60°, (c)0°, (d)60°, and (e)150°.

Fig. 5 shows the energy curve for the rotation of carboxyl group of threonine. The potential energy scan for the $-\text{COOH}$ group in threonine, defined by the dihedral angle between atoms 1N and 1O0 relative to bond 6C–3C, revealed highest energy conformers G (-100° ; $-275079.631 \text{ kcal}\cdot\text{mol}^{-1}$) and I (80° ; $-275073.327 \text{ kcal}\cdot\text{mol}^{-1}$). These correspond to gauche conformations between the $-\text{NH}_2$ nitrogen (1N) and the carboxyl oxygen (1O0), where close proximity of electronegative atoms results in strong repulsion. Lowest energy conformers F (-180°), H (-20°), and J (160°) had energies of $-275084.202 \text{ kcal}\cdot\text{mol}^{-1}$, $-275086.038 \text{ kcal}\cdot\text{mol}^{-1}$, and $-275084.559 \text{ kcal}\cdot\text{mol}^{-1}$, respectively, with conformer H stabilized by hydrogen bonding between atoms 1O0 and 2H (2.552 \AA).

For conformer H, the rotational barriers of $6.407 \text{ kcal}\cdot\text{mol}^{-1}$ (to G) and $12.711 \text{ kcal}\cdot\text{mol}^{-1}$ (to I) indicate significantly hindered rotation of the $-\text{COOH}$ group in threonine, consistent with prior DFT-based conformational studies reporting restricted carboxyl torsions in amino acids (Barone et al., 2023). Fig. 6 shows all the conformers.

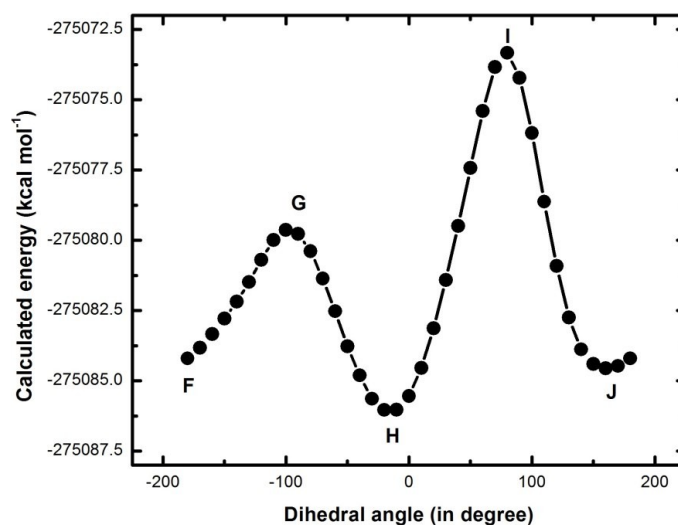


Fig. 5. Energy curve for the rotation of $-\text{COOH}$ group in threonine.

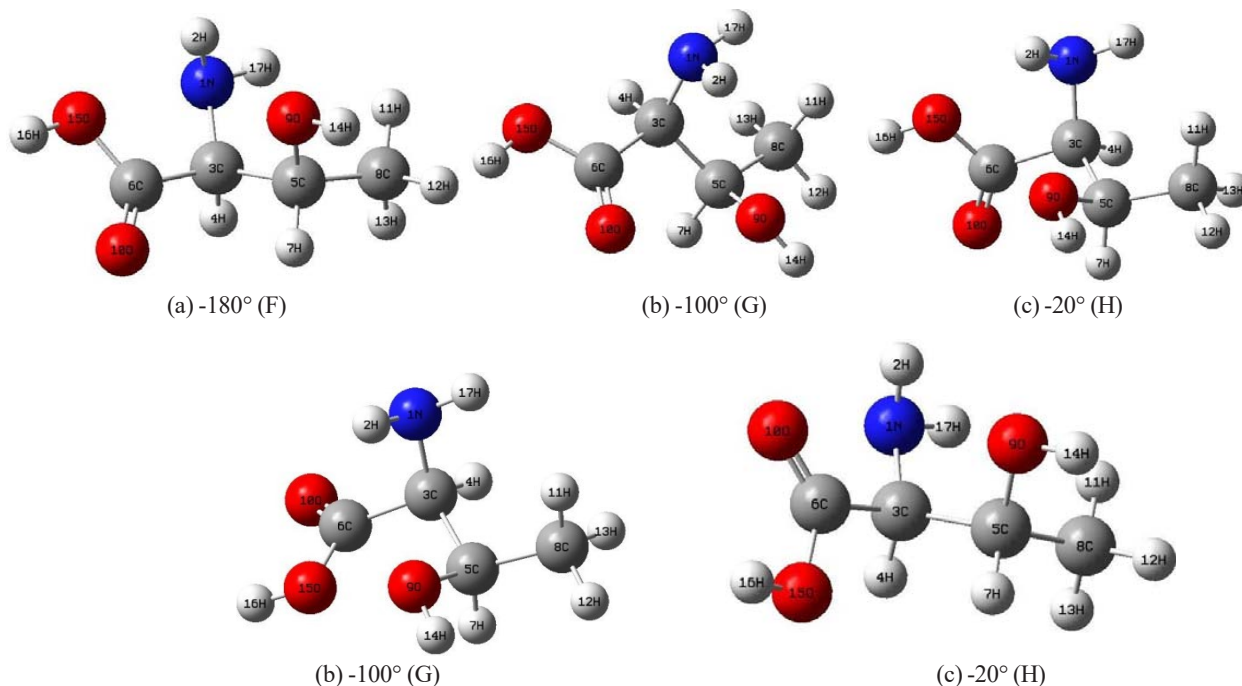


Fig. 6. Conformations obtained for the potential energy scan study of threonine while rotating -COOH group at different angles (a)-180°, (b)-100°, (c)-20°, (d)80°, and (e)160°.

Fig. 7 shows the energy curve for rotation of the $-\text{CH}(\text{CH}_3)\text{OH}$ side chain in threonine, defined by the dihedral angle between atoms 6C and 9O relative to bond 5C–3C, revealed four highest - energy conformers: K (-180° ; $-275078.560 \text{ kcal}\cdot\text{mol}^{-1}$), M (-110° ; $-275075.962 \text{ kcal}\cdot\text{mol}^{-1}$), O (20° ; $-275071.187 \text{ kcal}\cdot\text{mol}^{-1}$), and Q (130° ; $-275073.556 \text{ kcal}\cdot\text{mol}^{-1}$). Lowest-energy conformers were L (-160° ; $-275080.696 \text{ kcal}\cdot\text{mol}^{-1}$), N (-50° ; $-275079.835 \text{ kcal}\cdot\text{mol}^{-1}$), P (80° ; $-275078.824 \text{ kcal}\cdot\text{mol}^{-1}$), and R (180° ; $-275078.560 \text{ kcal}\cdot\text{mol}^{-1}$).

Rotational barriers for L were $2.136 \text{ kcal}\cdot\text{mol}^{-1}$ (to K) and $4.734 \text{ kcal}\cdot\text{mol}^{-1}$ (to M); for N, $3.873 \text{ kcal}\cdot\text{mol}^{-1}$ (to M) and $8.648 \text{ kcal}\cdot\text{mol}^{-1}$ (to O); and for P, $7.637 \text{ kcal}\cdot\text{mol}^{-1}$ (to O) and $5.268 \text{ kcal}\cdot\text{mol}^{-1}$ (to Q). These values indicate significantly hindered rotation. High-energy conformers O and Q arise from gauche interactions between 9O of $-\text{CH}(\text{CH}_3)\text{OH}$ and 15O of $-\text{COOH}$, leading to strong repulsion (Barone et al., 2023). The lowest-energy conformer L is stabilized by hydrogen bonding between 9O and 2H (2.397 \AA), while the second-lowest N is stabilized by multiple hydrogen bonds: 1N–11H (2.749 \AA), 9O–11H (2.694 \AA), and 15O–7H (2.653 \AA), lowering the total energy. The optimized geometries of these conformers are shown on Fig. 8.

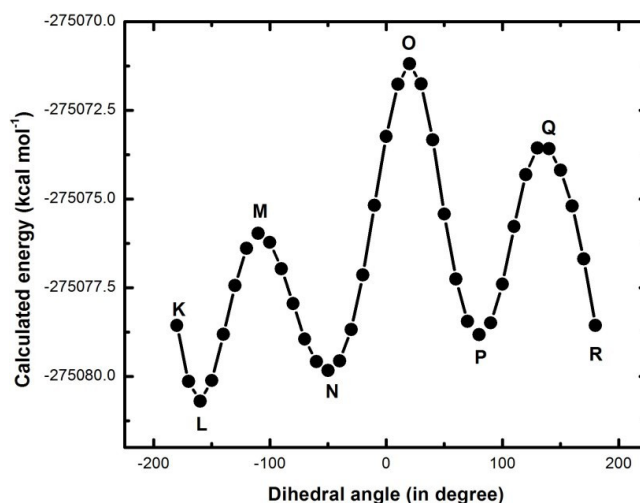


Fig. 7. Energy curve for the rotation of $-\text{CH}(\text{CH}_3)\text{OH}$ group in threonine.

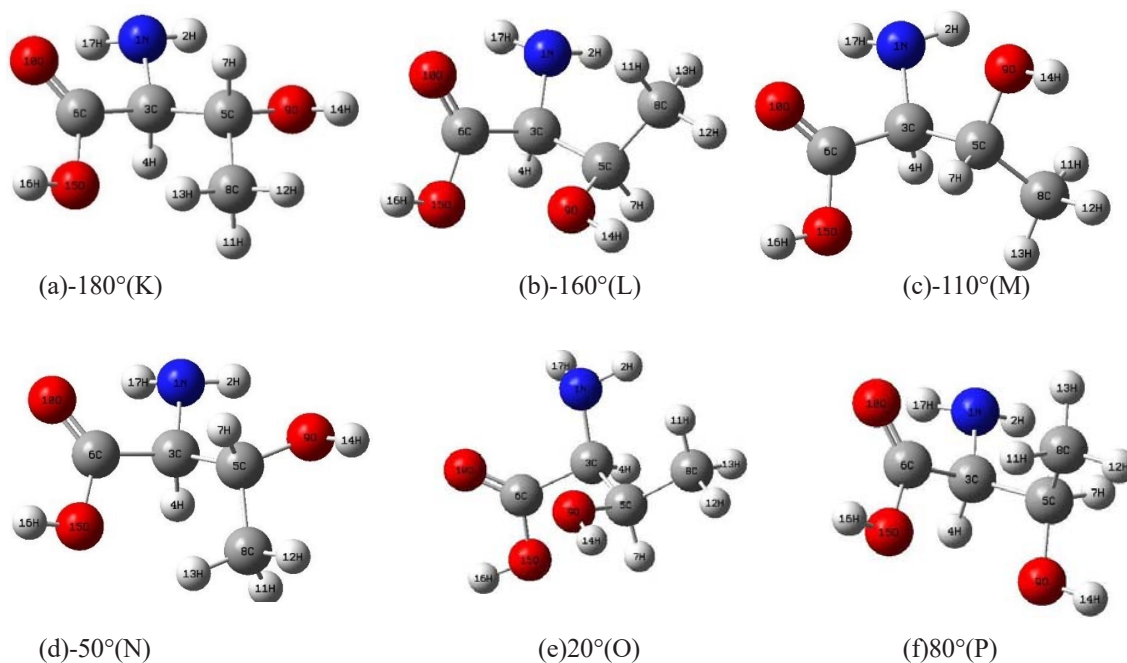


Fig. 8. Conformations obtained for the potential energy scan study of threonine while rotating $-\text{CH}(\text{CH}_3)\text{OH}$ group at different angles (a) -180° , (b) -160° , (c) -110° , (d) -50° , (e) -20° , (f) 80° , (g) 130° , and (h) 180° .

Conclusions

This study provides valuable insights into the structural characteristics of small amino acid sequences and their implications for overall protein stability. Geometry optimization of eight tripeptide combinations was performed at the DFT-B3LYP level using 6-31G* and 6-311G* basis sets, with detailed analysis of amide-plane and α -carbon geometries conducted at 6-311G*. Potential energy scans (PES) of the threonine residue for $-\text{NH}_2$, $-\text{COOH}$, and $-\text{CH}(\text{CH}_3)\text{OH}$ rotations were also carried out at the same theoretical level. Among the tripeptides studied, Methionine–Threonine–Phenylalanine exhibited the lowest optimization energy ($-1029809 \text{ kcal}\cdot\text{mol}^{-1}$), indicating the highest structural stability which is likely due to both the chemical nature and larger size of methionine. Comparative analysis of amide-plane bond lengths and angles revealed minimal variation across sequences, with maximum deviations of 0.053 \AA and 1.8° , respectively, suggesting these parameters are essentially fixed in protein chains. In contrast, α -carbon geometries showed notable deviations from the ideal tetrahedral angle (109.5°), with maxima of 4.4° (X-position) and 3.4° (Y-position), indicating residue-dependent distortions. Dihedral angle analysis further revealed non-planarity of amide planes, likely arising from hydrogen bonding between threonine residues and R-group atoms, as well as steric hindrance. PES results identified minimum-energy conformers and rotational energy barriers of $6.914 \text{ kcal}\cdot\text{mol}^{-1}$ ($-\text{NH}_2$), $12.711 \text{ kcal}\cdot\text{mol}^{-1}$ ($-\text{COOH}$), and $8.648 \text{ kcal}\cdot\text{mol}^{-1}$ ($-\text{CH}(\text{CH}_3)\text{OH}$). The higher barriers for $-\text{COOH}$ and $-\text{CH}(\text{CH}_3)\text{OH}$ indicate greater rigidity, with multiple minima in $-\text{CH}(\text{CH}_3)\text{OH}$ rotation further suggesting restricted mobility. Overall, these findings highlight the relative invariance of amide-plane geometry, the variability of α -carbon geometry, and the significant conformational constraints imposed by certain side-chain groups, all of which are critical for understanding protein chain stability. A limitation of this work is the use of only one functional (B3LYP), and future studies may benefit from including additional hybrid or meta-GGA functionals for comparison.

Acknowledgements

The authors thank the Department of Physics, Amrit Campus, for providing access to Gaussian 03 software and related computational support used in this study.

References

- Barone, V., Fusè, M., Lazzari, F., & Mancini, G. (2023). Benchmark structures and conformational landscapes of amino acids in the gas phase: A joint venture of machine learning, quantum chemistry, and rotational spectroscopy. *Journal of Chemical Theory and Computation*, 19(4), 1243-1260. <https://doi.org/10.1021/acs.jctc.2c01143>
- Barrett, G. C., & Elmore, D. T. (1998). *Amino acids and peptides*. Cambridge University Press.
- Berg, J. M., Tymoczko, J. L., & Stryer, L. (2007). *Biochemistry* (loose-leaf). Macmillan.
- Branden, C. I., & Tooze, J. (2012). *Introduction to protein structure* (2nd ed.). Garland Science.
- Chasse, G. A., Rodriguez, A. M., Mak, M. L., Deretey, E., Perczel, A., Sosa, C. P., Enriz, R. D., & Csizmadia, I. G. (2001). Peptide and protein folding. *Journal of Molecular Structure: THEOCHEM*, 537(1-3), 319-361. [https://doi.org/10.1016/S0166-1280\(00\)00687-4](https://doi.org/10.1016/S0166-1280(00)00687-4)
- Dennington, R. D., Keith, T. A., & Millam, J. M. (2008). GaussView 5.0.8. Gaussian, Inc, 340.
- Foresman, J., & Frisch, E. (1996). *Exploring chemistry*. Gaussian, Inc.
- Frisch, M. J., Trucks, G. W., Schlegel, H. B., Scuseria, G. E., Robb, M. A., Cheeseman, J. R., Scalmani, G., Barone, V., Mennucci, B., Petersson, G. A., Nakatsuji, H., Caricato, M., Li, X., Hratchian, H. P., Izmaylov, A. F., Bloino, J., Zheng, G., Sonnenberg, J. L., Hada, M., ... Fox, D. J. (2004). Gaussian 03, Revision E.01, Gaussian, Inc.
- Garrett, R. H. (2015). *Biochemistry*. Cengage Learning Canada Inc.
- Hardin, C., Pogorelov, T. V., & Luthey-Schulten, Z. (2002). Ab initio protein structure prediction. *Current Opinion in Structural Biology*, 12(2), 176-181. [https://doi.org/10.1016/S0959440X\(02\)00306-8](https://doi.org/10.1016/S0959440X(02)00306-8)
- Kaschner, R., & Hohl, D. (1998). Density functional theory and biomolecules: A study of glycine, alanine, and their oligopeptides. *The Journal of Physical Chemistry A*, 102(26), 5111-5116. <https://doi.org/10.1021/jp980975u>
- Lee, C., Yang, W., & Parr, R. G. (1988). Development of the Colle-Salvetti correlation-energy formula into a functional of the electron density. *Physical review B*, 37(2), 785. <https://doi.org/10.1103/PhysRevB.37.785>
- Lehninger, A. L., Nelson, D. L., & Cox, M. M. (2005). *Lehninger Principles of Biochemistry* (4th ed.). W.H. Freeman and Company.
- MacArthur, M. W., & Thornton, J. M. (1991). Influence of proline residues on protein conformation. *Journal of molecular biology*, 218(2), 397-412. [https://doi.org/10.1016/0022-2836\(91\)90721-H](https://doi.org/10.1016/0022-2836(91)90721-H)
- Mondal, S., Chowdhuri, D. S., Ghosh, S., Misra, A., & Dalai, S. (2007). Conformational study on dipeptides containing phenylalanine: a DFT approach. *Journal of Molecular Structure: THEOCHEM*, 810(1-3), 81-89. <https://doi.org/10.1016/j.theochem.2007.02.006>
- Pauling, L. (1960). *The nature of the chemical bond and the structure of molecules and crystals: an introduction to modern structural chemistry* (3rd ed.). Cornell university press.
- Ramachandran, G. N., Ramakrishnan, C., & Sasisekharan, V. (1963). Stereochemistry of polypeptide chain configurations. *Journal of Molecular Biology*, 7, 95-99. [https://doi.org/10.1016/s0022-2836\(63\)80023-6](https://doi.org/10.1016/s0022-2836(63)80023-6)
- Selvarengan, P., & Kollandaivel, P. (2004). Potential energy surface study on glycine, alanine and their zwitterionic forms. *Journal of Molecular Structure: THEOCHEM*, 671(1-3), 77-86. <https://doi.org/10.1016/j.theochem.2003.10.021>
- Sjöberg, B., Foley, S., Cardey, B., & Enescu, M. (2014). An experimental and theoretical study of the amino acid side chain Raman bands in proteins. *Spectrochimica Acta Part A: Molecular and Biomolecular Spectroscopy*, 128, 300-311. <https://doi.org/10.1016/j.saa.2014.02.080>
- Subedi, S. (2017). *Conformational study on various dipeptides and tripeptides containing cysteine: A DFT approach* (Master's dissertation, Tribhuvan University, Amrit Campus, Nepal).
- Voet, D., Voet, J. G., & Pratt, C. W. (2016). *Fundamentals of biochemistry: Life at the molecular level* (5th ed.). John Wiley & Sons.
- Wagner, I., & Musso, H. (1983). New naturally occurring amino acids. *Angewandte Chemie International Edition in English*, 22(11), 816-828. <https://doi.org/10.1002/anie.198308161>
- Yakubovich, A. V., Solov'yov, I. A., Solov'yov, A. V., & Greiner, W. (2006). Conformational changes in glycine tri- and hexapeptide. *The European Physical Journal D-Atomic, Molecular, Optical and Plasma Physics*, 39(1), 23-34. <https://doi.org/10.1140/epjd/e2006-00067-5>

Supplementary Information:

Table S1: Atomic numbering scheme for bond length variables (a – j) for eight tripeptides.

| Variable | Bond Type | Ala–Thr–Arg | Arg–Thr–Asn | Asn–Thr–Asp | Asp–Thr–Cys | Met–Thr–Phe | Thr–Thr–Thr | Lys–Thr–Met | Pro–Thr–Ser |
|----------|----------------------------------|-------------|-------------|-------------|-------------|-------------|-------------|-------------|-------------|
| a | C–N (amide linkage, X-group) | 17C–15N | 31C–29N | 29C–27N | 17C–15N | 17C–15N | 17C–15N | 17C–15N | 17C–15N |
| b | N–H (amide plane, X-group) | 15N–16H | 29N–30H | 27N–28H | 15N–16H | 15N–16H | 15N–16H | 15N–16H | 15N–16H |
| c | N–C (to central carbon, X-group) | 15N–6C | 29N–6C | 27N–6C | 15N–6C | 15N–6C | 15N–6C | 15N–6C | 15N–6C |
| d | C=O (amide carbonyl, X-group) | 6C–10O | 6C–10O | 6C–10O | 6C–10O | 6C–10O | 6C–10O | 6C–10O | 6C–10O |
| e | C–C (backbone, X-group) | 6C–3C | 6C–3C | 6C–3C | 6C–3C | 6C–3C | 6C–3C | 6C–3C | 6C–3C |
| f | C–C (amide linkage, Y-group) | 26C–25C | 16C–15C | 16C–15C | 28C–27C | 33C–32C | 30C–29C | 37C–38C | 30C–29C |
| g | C=O (amide carbonyl, Y-group) | 25C–27O | 15C–17O | 15C–17O | 27C–29O | 32C–34O | 29C–31O | 37C–39O | 29C–31O |
| h | C–N (amide plane, Y-group) | 25C–1N | 15C–1N | 15C–1N | 27C–1N | 32C–1N | 29C–1N | 37C–1N | 29C–1N |
| i | N–H (amide plane, Y-group) | 1N–2H | 1N–2H | 1N–2H | 1N–2H | 1N–2H | 1N–2H | 1N–2H | 1N–2H |
| j | N–C (to central carbon, Y-group) | 1N–3C | 1N–3C | 1N–3C | 1N–3C | 1N–3C | 1N–3C | 1N–3C | 1N–3C |

Table S2: Atomic numbering scheme for bond angle variables (I – XII) for eight tripeptides.

| Variable | Atoms | Ala–Thr–Arg | Arg–Thr–Asn | Asn–Thr–Asp | Asp–Thr–Cys | Met–Thr–Phe | Thr–Thr–Thr | Lys–Thr–Met | Pro–Thr–Ser |
|----------|-----------------|-------------|-------------|-------------|-------------|-------------|-------------|-------------|-------------|
| I | C–N–H (X-group) | 17C–15N–16H | 31C–29N–30H | 29C–27N–28H | 17C–15N–16H | 17C–15N–16H | 17C–15N–16H | 17C–15N–16H | 17C–15N–16C |
| II | C–N–C (X-group) | 17C–15N–6C | 31C–29N–6C | 29C–27N–6C | 17C–15N–6C | 17C–15N–6C | 17C–15N–6C | 17C–15N–6C | 17C–15N–6C |
| III | H–N–C (X-group) | 16H–15N–6C | 30H–29N–6C | 28H–27N–6C | 16H–15N–6C | 16H–15N–6C | 16H–15N–6C | 16H–15N–6C | 16C–15N–6C |
| IV | N–C–O (X-group) | 15N–6C–10O | 29N–6C–10O | 27N–6C–10O | 15N–6C–10O | 15N–6C–10O | 15N–6C–10O | 15N–6C–10O | 15N–6C–10O |
| V | N–C–C (X-group) | 15N–6C–3C | 29N–6C–3C | 27N–6C–3C | 15N–6C–3C | 15N–6C–3C | 15N–6C–3C | 15N–6C–3C | 15N–6C–3C |

| | | | | | | | | | |
|------|--------------------|-------------|-------------|-------------|-------------|-------------|-------------|-------------|-------------|
| VI | O–C–C (X-group) | 10O–6C–3C | 10O–6C–3C | 10O–6C–3C | 10O–6C–3C | 10O–6C–3C | 10O–6C–3C | 10O–6C–3C | 10O–6C–3C |
| VII | C–C–O (Y-group) | 26C–25C–27O | 16C–15C–17O | 16C–15C–17O | 28C–27C–29O | 33C–32C–34O | 30C–29C–31O | 38C–37C–39O | 30C–29C–31O |
| VIII | C–C–N (Y-group) | 26C–25C–1N | 16C–15C–1N | 16C–15C–1N | 28C–27C–1N | 33C–32C–1N | 30C–29C–1N | 38C–37C–1N | 30C–29C–1N |
| IX | O–C–N (Y-group) | 27O–25C–1N | 17O–15C–1N | 17O–15C–1N | 29O–27C–1N | 34O–32C–1N | 31O–29C–1N | 39O–37C–1N | 31O–29C–1N |
| X | C–N–H (Y-group) | 25C–1N–2H | 15C–1N–2H | 15C–1N–2H | 27C–1N–2H | 32C–1N–2H | 29C–1N–2H | 37C–1N–2H | 29C–1N–2H |
| XI | C–N–C (Y-group) | 25C–1N–3C | 15C–1N–3C | 15C–1N–3C | 27C–1N–3C | 32C–1N–3C | 29C–1N–3C | 37C–1N–3C | 29C–1N–3C |
| XII | H–N–C (Y-group) | 2H–1N–3C | 2H–1N–3C | 2H–1N–3C | 2H–1N–3C | 2H–1N–3C | 2H–1N–3C | 2H–1N–3C | 2H–1N–3C |

Table S3: Atomic numbering scheme for α -carbon bond angle variables (k – p) for eight tripeptides.

| Variable | Atoms | Ala–Thr–Arg | Arg–Thr–Asn | Asn–Thr–Asp | Asp–Thr–Cys | Met–Thr–Phe | Thr–Thr–Thr | Lys–Thr–Met | Pro–Thr–Ser |
|----------|--|---|---|---|---|---|---|---|---|
| k | N–C _{α} –C (X-group) | 15N–17C _{α} –19C | 29N–31C _{α} –33C | 27N–29C _{α} –31C | 15N–17C _{α} –19C | 15N–17C _{α} –20C | 15N–17C _{α} –20C | 15N–17C _{α} –19C | 15N–17C _{α} –23C |
| l | N–C _{α} –H (X-group) | 15N–17C _{α} –18H | 29N–31C _{α} –32H | 27N–29C _{α} –30H | 15N–17C _{α} –18H | 15N–17C _{α} –18H | 15N–17C _{α} –18H | 15N–17C _{α} –18H | 15N–17C _{α} –22H |
| m | N–C _{α} –C (X-group) | 15N–17C _{α} –20C | 29N–31C _{α} –34C | 27N–29C _{α} –32C | 15N–17C _{α} –20C | 15N–17C _{α} –19C | 15N–17C _{α} –19C | 15N–17C _{α} –19C | 15N–17C _{α} –21C |
| n | C–C _{α} –N (Y-group) | 25C–26C _{α} –28N | 15C–16C _{α} –18N | 15C–16C _{α} –18N | 27C–28C _{α} –30N | 32C–33C _{α} –35N | 29C–30C _{α} –32N | 37C–38C _{α} –40N | 29C–30C _{α} –32N |
| o | C–C _{α} –H (Y-group) | 25C–26C _{α} –29H | 15C–16C _{α} –19H | 15C–16C _{α} –19H | 27C–28C _{α} –31H | 32C–33C _{α} –36H | 29C–30C _{α} –33H | 37C–38C _{α} –41H | 29C–30C _{α} –33H |
| p | C–C _{α} –C (Y-group) | 25C–26C _{α} –30C | 15C–16C _{α} –20C | 15C–16C _{α} –20C | 27C–28C _{α} –32C | 32C–33C _{α} –37C | 29C–30C _{α} –34C | 37C–38C _{α} –42C | 29C–30C _{α} –34C |

Table S4: Atomic numbering scheme for dihedral angles for eight tripeptides.

| Variable | Atoms / Reference bond | Ala–Thr–Arg | Arg–Thr–Asn | Asn–Thr–Asp | Asp–Thr–Cys | Met–Thr–Phe | Thr–Thr–Thr | Lys–Thr–Met | Pro–Thr–Ser |
|-----------------|-------------------------------|------------------|------------------|------------------|------------------|------------------|------------------|------------------|------------------|
| D _{Nx} | X-group dihedral (C–H / N–C) | 17C–16H / 15N–6C | 31C–30H / 29N–6C | 29C–28H / 27N–6C | 17C–16H / 15N–6C | 17C–16H / 15N–6C | 17C–16H / 15N–6C | 17C–16H / 15N–6C | 17C–16H / 15N–6C |
| D ₁ | N–O dihedral wrt C–C backbone | 15N–10O / 6C–3C | 29N–10O / 6C–3C | 27N–10O / 6C–3C | 15N–10O / 6C–3C | 15N–10O / 6C–3C | 15N–10O / 6C–3C | 15N–10O / 6C–3C | 15N–10O / 6C–3C |
| D ₂ | C–C dihedral wrt N–C backbone | 17C–3C / 15N–6C | 31C–3C / 29N–6C | 29C–3C / 27N–6C | 17C–3C / 15N–6C | 17C–3C / 15N–6C | 17C–3C / 15N–6C | 17C–3C / 15N–6C | 17C–3C / 15N–6C |
| D ₃ | H–C dihedral wrt N–C backbone | 16H–3C / 15N–6C | 30H–3C / 29N–6C | 28H–6C / 27N–6C | 16H–3C / 15N–6C | 16H–3C / 15N–6C | 16H–3C / 15N–6C | 16H–3C / 15N–6C | 16H–3C / 15N–6C |
| D _{Ny} | Y-group dihedral (C–H / N–C) | 3C–2H / 1N–25C | 3C–2H / 1N–15C | 3C–2H / 1N–15C | 3C–2H / 1N–27C | 3C–2H / 1N–32C | 3C–2H / 1N–29C | 3C–2H / 1N–37C | 3C–2H / 1N–29C |

| | | | | | | | | | |
|----------------|-----------------------------------|---------------------|---------------------|---------------------|---------------------|---------------------|---------------------|---------------------|---------------------|
| D ₄ | Y-group N-O torsion wrt C-C | 1N-27O / 25C-26C | 1N-17O / 15C-16C | 1N-17O / 15C-16C | 1N-29O / 27C-28C | 1N-34O / 32C-33C | 1N-31O / 29C-30C | 1N-39O / 37C-38C | 1N-31O / 29C-30C |
| D ₅ | Y-group C-C torsion wrt N-C | 3C-26C / 1N-25C | 3C-16C / 1N-15C | 3C-16C / 1N-15C | 3C-28C / 1N-27C | 3C-33C / 1N-32C | 3C-30C / 1N-29C | 3C-38C / 1N-37C | 3C-30C / 1N-29C |
| D ₆ | Y-group H-C torsion wrt N-C | 2H-26C / 1N-25C | 2H-16C / 1N-15C | 2H-16C / 1N-15C | 2H-28C / 1N-27C | 2H-33C / 1N-32C | 2H-30C / 1N-29C | 2H-38C / 1N-37C | 2H-30C / 1N-29C |